THE UNIVERSITY OF MICHIGAN BUBBLE CHAMBER PROGRAM*

J. L. BROWN, C. DODD, D. A. GLASER and M. L. PERL

University of Michigan, Ann Arbor (Mich.)

and

D. C. RAHM

Brookhaven National Laboratory, Upton (N.Y.)

(presented by D. A. Glaser)

General remarks about bubble chambers

Less than four years ago the first track of a charged particle was obtained in a tiny glass bubble chamber. The apparatus contained only a few cubic centimeters of hot diethyl ether, and was extremely crude and simple. Since then physicists in more than twenty-five laboratories in different countries have constructed a large variety of chambers using a wide assortment of working liquids. Tracks have been photographed in helium, hydrogen, ethylene, xenon, propane, butane, pentane, diethyl ether, and probably other liquids. In addition it has been demonstrated that sulfur dioxide, benzene, ethyl alcohol, methyl alcohol, and nitrogen are radiation sensitive. Indeed every liquid that has been tried extensively (except beer, which was used in the first hasty attempt), has been shown to be workable if the experimenter is willing to maintain the required pressures and temperatures. Even beer (i.e. water) should work at sufficiently high temperatures and pressures.

A great variety of chambers has been constructed and designed for future construction. They range in size from a xenon chamber one inch in diameter to a hydrogen chamber which is to be 72 inches long and operate in a magnetic field of 20,000 gauss. Most of these chambers are intended to use with pulsed accelerators, but some are to be used for cosmic ray experiments by means of random expansions. Unfortunately the hydrocarbon bubble chambers have been shown experimentally to be incapable of counter-controlled operation because of the shortness of the lifetime of the "latent image". Our present view of the basic process underlying bubble chamber operation leads us to expect that no bubble chamber will be able to operate successfully by means of counter-controlled expansions. Certain types of very high energy accelerators now being considered produce continuous rather than pulsed beams. If bubble chambers are to be used with these machines, random expansions will probably be required.

Two main types of bubble chambers are in current use. Chambers constructed entirely of glass fused into one piece are termed "clean" chambers, because their walls are smooth and clean so that boiling usually begins within the liquid rather than at the walls. Chambers fabricated of metals, gaskets, and glass are called "dirty" chambers. Boiling always begins first at the walls or joints of "dirty" chambers. Clean chambers have a somewhat longer sensitive time after each random expansion, at least for small chambers, and require somewhat lower temperatures and pressures for operation with a given liquid. Bubbles grow faster in clean chambers because of the larger pressure drop which can be attained in their operation (even negative pressures can be used). For extremely low temperature operation the all-glass construction of clean chambers simplifies some of the technical problems, especially for small chambers.

Dirty chambers have the great advantage that they can readily be built in large sizes with windows of good optical quality. Their sensitive time is long enough for operation with pulsed accelerators, and the growth of their bubbles is slow enough to allow good quality tracks to be obtained over a fairly long time interval. On the other hand the bubbles grow fast enough that bubble sizes can be used to estimate the ages of tracks in a dirty chamber. This is important for establishing the association between related events not connected by an ionizing link in a bubble chamber photograph.

Since many of these points will be discussed in detail by other speakers, I will spend the rest of my time describing

* Work supported partly by the National Science Foundation and the U. S. Atomic Energy Commission.

recent developments in our laboratory at the University of Michigan. One of our main results this year is the establishing of bubble counting as a technique for measuring charged particle velocities.

Another result is the successful operation of a liquid xenon bubble chamber. The main advantage of this chamber is its high efficiency in detecting neutral pi mesons and gamma rays.

Another result is the successful operation of a liquid xenon bubble chamber. The main advantage of this chamber is its high efficiency in detecting neutral pi mesons and gamma rays.

Since bubble chambers can be operated to record events at every pulse of a large accelerator, photographs will be collected very rapidly. A sizeable fraction of the photographs of a large bubble chamber will contain events worthy of quantitative analysis. This time-consuming analysis will probably be the bottle-neck in utilizing bubble chamber data since finding interesting events should be relatively easy. We have therefore developed a semi-automatic method of analysis. The steps in this method are the following.

1. Coordinates of corresponding points will be measured on the two stereographic negatives by means of a projection comparator containing motor-driven precision lead screws.

2. These film coordinates will be recorded automatically on punched cards.

3. A high speed electronic computer will compute the correct three-dimensional coordinates of the original point using sterescopic formulas including corrections for the high index of refraction of the thick glass windows and the chamber liquid.

4. Precision grids in the chamber will appear in each photograph to provide a basis for eliminating optical and film distortions.

5. Track lengths, angles between tracks, magnetic curvatures, and mean scattering angles will be found by the computer using these true coordinates.

6. Momenta and energies will be computed for various possible particle assignments tried in order by the computer.

By this method we hope to eliminate much of the tedium of data analysis and gather information about nuclear physics at a rate commensurate with the great cost and difficulty of constructing large accelerators and associated experimental apparatus.

A liquid xenon bubble chamber *

A particle detector capable of detecting gamma rays with high efficiency in addition to giving accurate information concerning the paths, velocities, and energies of charged particles should be of great value in studies of elementary particles and high energy nuclear phenomena. It was pointed out by one of us [1] that a bubble chamber filled with a liquid of high density and large atomic number would have these properties. Of a number of possible liquids, xenon seemed the most promising because it is non-toxic, non-corrosive, chemically stable, and was expected to require convenient pressures and temperatures for bubble chamber operation.

The investigation of xenon as a filling liquid for bubble chambers was carried out in an aluminium chamber with a sensitive volume one inch in diameter and one-half inch deep along the camera axis. The expansion mechanism, photographic apparatus and chamber construction were closely similar to those of bubble chambers already described[2], except that the temperature of the circulating air was maintained by dry ice cooling. The measurements of the temperature of the liquid inside the chamber were indirect and may be in error by as much as two degrees C.

As a preliminary test of the operation of the entire system, the chamber was filled with ethylene which has a vapor pressure curve almost identical with that of xenon in the range of temperatures of interest here. Fig. 1 shows the tracks of electrons produced in ethylene by gamma rays from a 100 mc. radium beryllium source held 8 inches from the center of the chamber, when the chamber was at – 18 degrees C.

When the chamber was filled with liquid xenon and run under closely similar conditions immeditely after the ethylene experiments, no tracks were obtained. The chamber was then altered in an attempt to produce tracks in xenon by enlarging the expansion channel to expand the chamber faster and by replacing the original teflon gaskets and diaphragm by buthyl rubber to avoid the excessive absorption of xenon exhibited by the teflon. Still no tracks could be seen.

Shortly after these failures to observe tracks, we learned [3] that gaseous xenon had been found to be an efficient scintillating material, so that some sizeable fraction of the energy lost by an ionizing particle in liquid xenon might escape in optical radiation instead of being deposited locally in the xenon itself. Other experiments recently completed in this laboratory [4] seemed to indicate that the operation of a bubble chamber depends upon the local deposition and thermalization in the liquid of energy from the ionizing particle. To capture locally the energy which was escaping in optical radiation, we dissolved some

* Brown, J. L., Glaser, D. A., and Perl, M. L. Phys. Rev. *102*, p. 586—7, 1956.

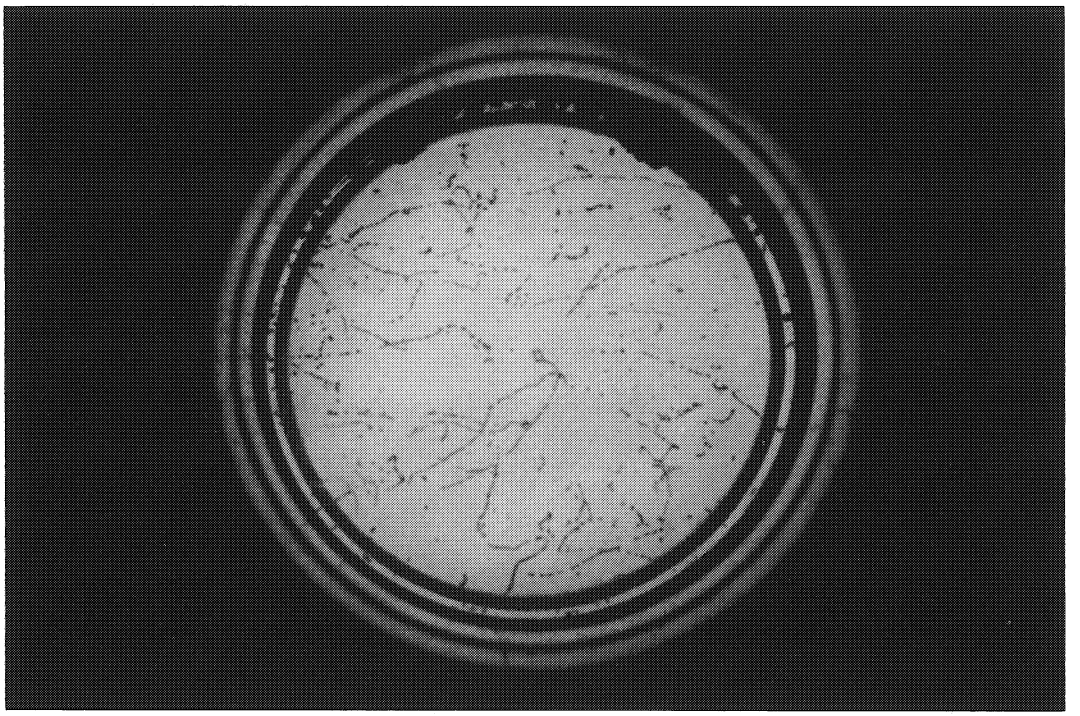

Fig. 1. Tracks of Compton electrons produced by γ rays from a 100 mc. radium beryllium source placed 8 inches from the center of a bubble chamber one inch in diameter filled with liquid ethylene at -18 °C. The density of the liquid is about 0.5 g/cm³. The duration of the light flash is 5 microseconds and the flash occurred 3 milliseconds after the expansion was initiated.

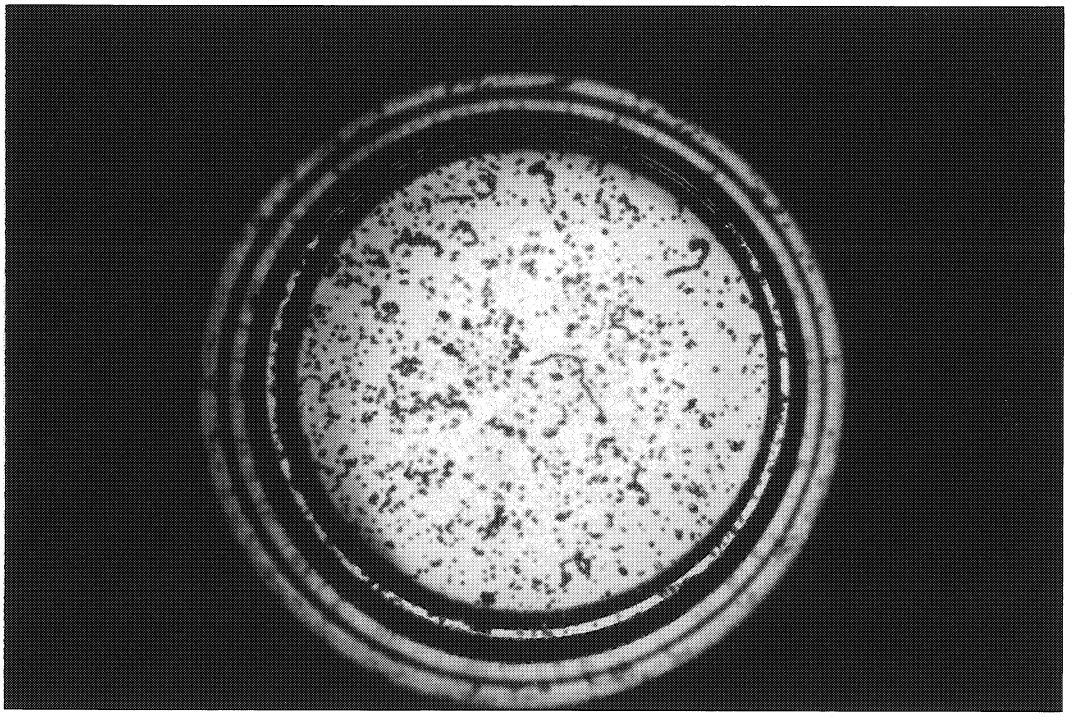

Fig. 2. Tracks of Compton electrons produced by γ rays from a 25 cm. radium beryllium source placed 8 inches from the center of the same chamber filled with liquid xenon containing 2% by weight of ethylene and operated at -19 °C. The density of the liquid is about 2.3 gm/cm³ and the lighting conditions are the same as in fig. 1.

ethylene in the liquid xenon in the hope that it would "quench" the scintillation effect by collisions of the second kind. With less than 2% by weight of ethylene, the bubble chamber became radiation sensitive and produced copious tracks of electrons when exposed to a 25 mc. radium beryllium source of gamma rays as shown in fig. 2. A large number of picturesve been ha taken of this xenon chamber and indicate that the track formation is reasonably insensitive to the temperature and to the proportion of ethylene.

As a particle detector the xenon bubble chamber has properties similar to those of nuclear emulsion. The density of the liquid is 2.3 g/cm^3, the radiation length is 3.1 cm., and the Coulomb scattering constant is about the same as that of emulsion. Since the accuracy of scattering measurements increases as $L^{3/2}$, if L is the length of track measured, the xenon bubble chamber should yield useful scattering measurements because of the long track lengths possible, even though the accuracy of determining coordinates of points on a track is less by at least a factor ten than for emulsions. There is no basic limit on the possible size of xenon bubble chambers for use with pulsed accelerators. It competes in cost with large emulsion stacks because the liquid can be used indefinitely for many experiments. The main advantages of the xenon bubble chamber are that scanning of the photographs is easy and gamma rays can be detected efficiently by their production of compton electrons at low gamma energies and electron pairs at high energies. Association of these gamma rays with their parent events should be easy because of the very low background of events per picture in bubble chambers, and the very rapid bubble growth which allows simultaneity of events to be estimated by bubble size to less than a millisecond. It should therefore be possible using a xenon bubble chamber to study directly those decay modes of unstable particles involving gamma rays and neutral pions, which decay rapidly in flight into gamma rays, and other nuclear processes in which gamma rays are emitted. It should be possible to determine the energies of gamma rays by multiple scattering measurements of the electron pairs.

We would like to thank Dr. Cyril Dodd and Messrs. C. Graves and L. O. Roellig for help in making some of the early runs.

The Linde Air Products Company generously donated to the University of Michigan the xenon used in our experiments.

Note : After our experiments were completed, we learned in a telephone conversation with Dr. Keith Boyer of the Cyclotron Group at the Los Alamos Scientific Laboratory that the high speed and scintillation efficiency of xenon gas depends only very slightly on pressure from a few millimeters of mercury up to 3 atmospheres. A small admixture of a few tenths of a percent of gaseous hydrocarbon, however, is found to practically destroy the scintillation effects ! If the same mechanism is at work in the scintillation "quenching" as in the xenon bubble chamber, we might expect the large scintillation efficiency of xenon to extend to the liquid state at – 20 °C and 20 atmospheres of pressure.

It seems rather remarkable that the same effect should be found under such different thermodynamic conditions. Perhaps it will be possible to adjust the percentage of hydrocarbon admixture so that the liquid xenon retains some of its scintillating efficiency and also produces bubble tracks. Then one might be able to observe spatial as well as temporal data for each nuclear process of interest. Thus decay times of particles, for example, could be associated with their identity as revealed by their daughter particles, etc.

Bubble counting for the determination of the velocities of charged particles in bubble chambers *

I. *Introduction*

An important feature of the cloud chamber and nuclear emulsion for interpretation of nuclear processes is their ability to furnish information concerning particle velocities by measurement of the relative ionization. Together with other data, this ionization measurement permits the identification of particles, the determination of particle masses, and the calculation of characteristics of nuclear events.

The usefulness of the bubble chamber as a research instrument in nuclear physics is similarly much enhanced by the experimental finding that the density of bubbles along a track is a quantitative measure of the velocity of charged particles. Previously published bubble chamber photographs demonstrated this possibility qualitatively [2], but now we have completed a systematic series of measurements which establishes the quantitative reliability of bubble counting as a technique analogous to grain counting in a nuclear emulsion or droplet counting in a cloud chamber. The bubble density measured in propane did not turn out to be proportional to the relative ionization, but rather is a linear function of $1/\beta^2$, where $\beta = v/c$ is the relativistic velocity of the particle. This result makes it seem likely that some of the bubbles are produced by low energy delta rays along the track, since their number is proportional to $1/\beta^2$. All of the bubbles observed in these experiments cannot be explained this simply. A complete explanation of the observed bubble densities will probably require a detailed study of the properties of superheated liquids.

* Glaser, D. A., Rahm, D. C. and Dodd, C. Phys. Rev. *102*, p. 1653—8, 1956.

II. *Experimental method*

To establish the relationship between the velocity of a singly-charged particle and the density of bubbles along its track, we took photographs of a beam consisting mainly of protons and positive pions passing through the Michigan six-inch bubble chamber [2, 5] filled with liquid propane. This beam was produced by the Brookhaven Cosmotron by allowing the internal 3 Bev proton beam to strike a graphite target. Particles emerging at an angle of 32° with respect to the circulating proton beam were allowed to pass through an opening in the concrete shielding wall, a gap in an exterior steering magnet, and finally the bubble chamber. By adjusting the current in the steering magnet, particles of any chosen momentum could be made to pass through the bubble chamber. A schematic diagram of the experimental arrangement is shown in fig. 3. The bubble chamber was originally placed about 11 feet from the center of the magnet and the beam was deflected through an angle of about 19° with a maximum momentum of 1.6 Bev/c. When analysis of some of the early pictures indicated that the momentum resolution was not as good as was needed, the bubble chamber was moved to a position about 42 feet from the center of the magnet and the beam was deflected through an angle of about 32° with a maximum momentum of 915 Mev/c.

Absolute momentum calibration was done by the hot wire method with an error of less than 2%. During the later runs the magnet current was held constant within $^1/_2$%. The momentum resolution due to the width of the channels that defined the beam is estimated to have been about 6% for the first position and 2% for the second position. Scattering due to the long air path in the second location would add another 1% error for low momentum particles. Scattering from collimator walls and magnet pole tips would contribute a few particles with widely varying momenta, but selection of parallel particles in the bubble chamber eliminated most of these.

Since the sensitive time of the six-inch bubble chamber is only 2 to 3 milliseconds, it is important that the particles arrive during this rather narrow time interval. The Cosmotron output beam has a duration of about 3 milliseconds with a time uncertainty of one millisecond with respect to its master timing system. Since the main part of the beam comes out in one millisecond, it was possible to guarantee catching a sufficient number of particles by flashing the lights for photographing the chamber just after the maximum beam intensity occurred, using a scintillation counter telescope to monitor the beam. This assured us of getting substantial numbers of particles traversing the chamber during the period of uniform sensitivity. Particles arriving at other times will have anomalously low bubble densities as will be discussed below. For the best results using bubble chambers with large accelerators, it is therefore desirable to have beam pulses of very short duration.

Some difficulty was experienced in maintaining the temperature of the chamber constant, because the mechanical work done on the liquid during recompression added a few watts of heat to the liquid during extended runs. Temperatures were maintained stable to about 0.1 °C. during each run at a given momentum, though the thermistor-controlled oven temperature was more closely controlled. Also the temperature uniformity across the chamber was much better than 0.1 °C.

Each picture contained up to 20 countable tracks, some of which were minimum ionizing pions and some protons ionizing more heavily. Their momenta ranged from 530 Mev/c to 1.6 Bev/c. Some minimum ionizing tracks appeared in practically every picture so that we could

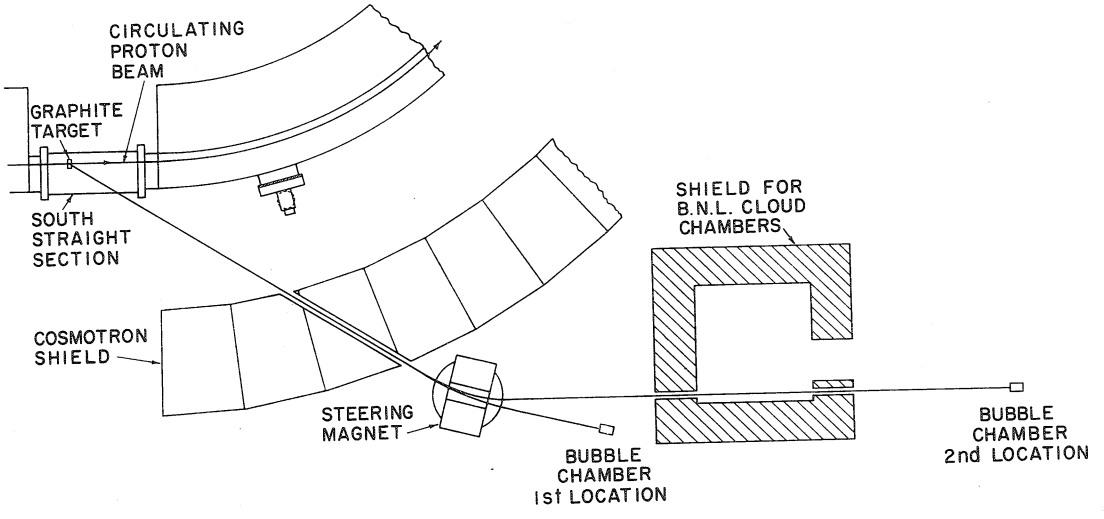

Fig. 3. From the particles produced by the 3 Bev circulating proton beam on striking the graphite target, positive pions and protons in the momentum range 530 Mev/c to 1600 Mev/c are selected. At the first bubble chamber location, 11 feet from the steering magnet, the total spread in momentum is about 6%; at the second location, 42 ft. away from the steering magnet, the spread is about 3%.

check ratios of bubble densities against relative ionizations and velocities as well as the absolute values of these quantities. The bubble densities were measured for tracks having different rates of energy loss ranging from the minimum value up to about four times minimum. Most of the measurements in propane were done at 55.5 °C., 56.5 °C., 57.5 °C., and 59.5 °C., although a few measurements were made at 50 °C., 52 °C., 53 °C., 54 °C., and 55 °C.

III. *Measurements and corrections*

Measurements were made by aligning the image of a track on the negative with the precision motion of a travelling microscope and counting the bubbles as their images were moved slowly across the center of the field of view. Bubble densities up to about 150 bubbles per centimeter on the negative could be counted with negligible error due to fusion of neighboring bubble images. Since the average photographic demagnification was 2.5, this corresponds to 60 bubbles per centimeter on the original track. This limitation is essentially optical, arising from the fact that the smallest bubble images on the negative are 40 microns in diameter as a result of diffraction and depth of field effects.

Only those tracks which were found by stereoscopic inspection to be closely parallel to the expected beam direction were accepted for measurement. In this way most of the particles scattered by the collimators and chamber walls were eliminated from consideration. In addition, the true lengths of the measured track segments were obtained by making a correction for the variation of magnification with depth. This correction amounted to about 3% in the final bubble densities.

The most important correction by far arises from the fact that each photograph contains tracks of various ages because the beam pulse is several milliseconds long. A number of tracks were found to have fewer bubbles than expected even for minimum ionizing particles. Since these tracks always consisted of abnormally large bubbles, it was concluded that they were old tracks formed during the early phase of the expansion of the chamber before it was fully sensitive. The existence of such a phase of incomplete sensitivity has already been established experimentally [2, 5]. By eliminating all tracks whose bubble images were larger than 0.100 mm. in diameter, all the "sub-minimum" tracks were eliminated and the histograms displaying the results became much more sharply peaked. The choice of the largest admissible bubble size which gives reliable bubble counts depends on the relative timing of the beam pulse and the lights and slightly on the temperature. This limiting size can be determined easily for a given experimental arrangement by counting bubbles on a few minimum ionizing tracks of various bubble sizes.

Finally the incident energy of the particles was corrected for the energy loss in the walls of the oven and the chamber, and for half the loss in the propane. The small error made by averaging the bubble density over the whole track of a particle which is slowing down slightly, is not serious in most of the cases considered in detail here. For the few cases of stopping particles which were measured, bubbles were counted for only a small portion of the total visible track length.

IV. *Results*

When straight parallel beam tracks of small bubbles are selected and the measured bubble densities corrected as described in the last section, the resulting bubble densities corresponding to a single momentum value fall into two main groups as shown by the typical histogram in fig. 4. Pion tracks of initial momentum 915 Mev/c contain about 200 bubbles and proton tracks of the same momentum contain about 340 for tracks about 12.5 centimeters long at 55.5 °C. Assuming the bubbles to result from statistically independent events, the corresponding errors resulting from fluctuations in the total number of bubbles on a track are 7% and 5.4% for a single track of this length. From the final form of the relationship between bubble density and particle velocity, we conclude that the spread in momentum of the particles used for this measurement contributes as much as 3% error in bubble density for the slower particles, and not at all for the fastest.

The resulting error of 8 or 9% is consistent with the width of the peaks in fig. 4, so we can expect the accuracy of our measurements on single unknown tracks to be limited mainly by the statistical fluctuations in the number of bubbles formed, counting errors being negligible. For

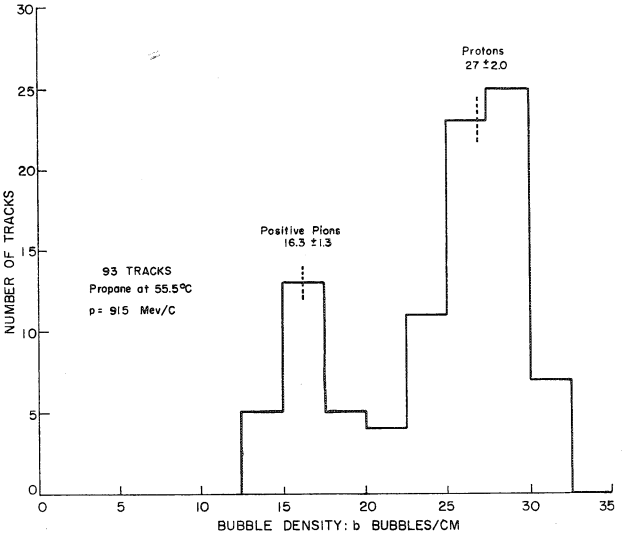

Fig. 4. Histogram showing the relative frequency of measured corrected bubble densities. The incident beam contained protons and positive pions of momentum 915 ± 30 Mev/c. The liquid is propane at 55.5 °C. In the propane the relativistic velocities are $\beta = 0.676$ for the protons and $\beta = 0.988$ for the pions. The protons are losing energy at 1.64 times the minimum energy loss.

bubble densities exceeding 60 bubbles per centimeter, however, fusion of neighboring bubbles, or, more likely, bubble images, begins to limit the counting accuracy. Since all of the images are along the line of the track, and not diffused as are droplet images on cloud chamber tracks, photoelectric bubble counting may be possible. To investigate its feasibility we have made microphotometer traces of the negatives for tracks of various bubble sizes and densities. The results make it seem promising to try photoelectric bubble counting. Aside from the obvious labor-saving advantages, an automatic method might make possible some reproducible way of counting fused and almost fused images so that a reliable empirical calibration can be established, even if each individual bubble is not counted. Human observers vary in their judgement of fused images and give an unreproducible error in counting dense tracks.

The measured bubble densities are found to depend rather sharply on the temperature as shown in fig. 5. From these curves one can estimate the temperature stability required to maintain a given maximum error in bubble density. In propane at 56 °C., temperature stability of about 0.1 °C. is needed to hold the bubble density constant within 2% for $1/\beta^2$ lying between 1 and 3.3.

From measurements of the thermodynamic conditions required for bubble nucleation in several liquids exposed to various radiations [4], and from theoretical ideas concerning the microscopic mechanism of the process [6], we have concluded that bubbles are nucleated along the path of a charged particle by local deposit of energy in the liquid by delta rays. We therefore did not expect to find that the bubble density is proportional to the relative ionization of the particle, but rather that it depends on the delta ray density. Fig. 6 shows that the bubble density is not a linear function of relative ionization, especially at large values of the ionization.

The number of delta rays in a given energy range produced by a charged particle flying through the liquid can be calculated by integrating the collision cross-section for the moving particle against free electrons over the chosen range of energies of the ejected electrons. Using known cross-sections [7] one finds that relativistic terms and terms dependent on particle spin contribute less than one per cent for the cases of interest here. The resulting number of delta rays whose energies lie between E'_1 and E'_2 electron-volts is

$$n_\delta = \frac{1.53 \times 10^5 \frac{Z}{A}}{\beta^2}\left[\frac{1}{E'_1} - \frac{1}{E'_2}\right] \mathrm{gm}^{-1}\,\mathrm{cm}^2 \qquad (1)$$

where Z and A are the charge and mass numbers of the

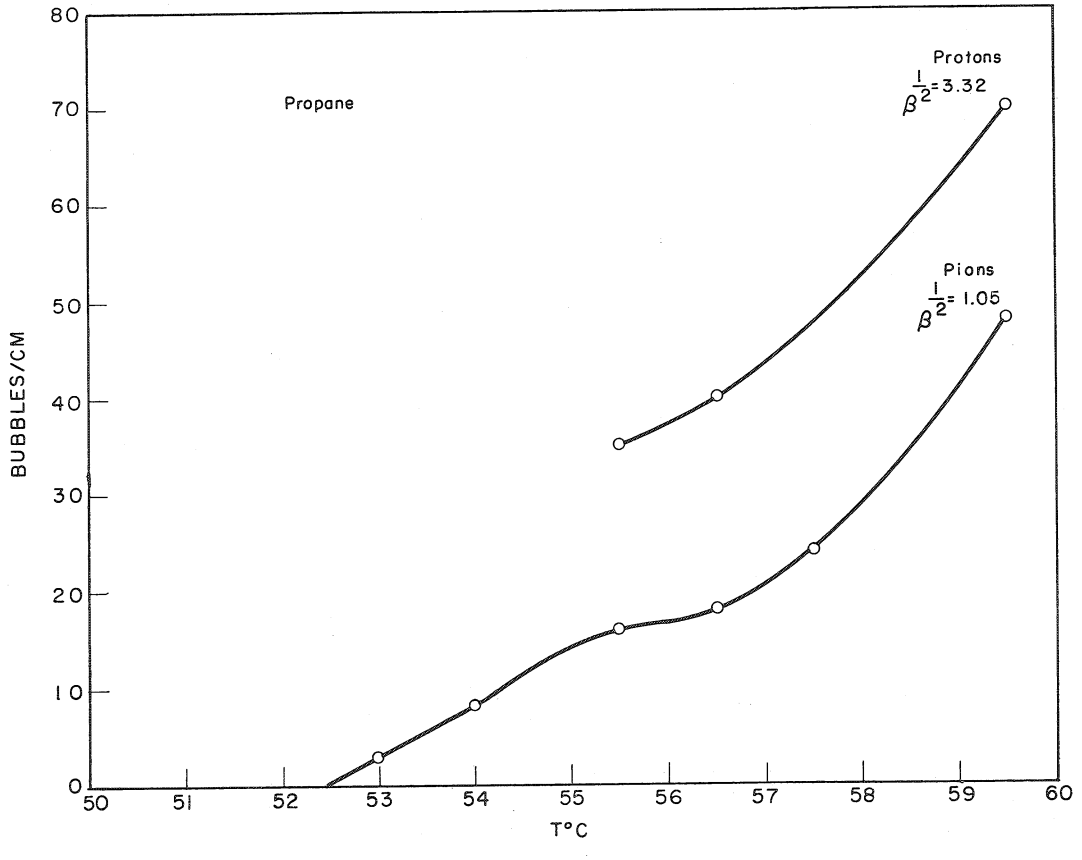

Fig. 5. Observed bubble density in propane versus temperature for pions with $1/\beta^2 = 1.05$ and protons with $1/\beta^2 = 3.32$. The total track lengths measured are sufficient to reduce statistical errors below 2% in bubble density. The momentum spread in the proton beams contribute an error of about 3% in bubble density.

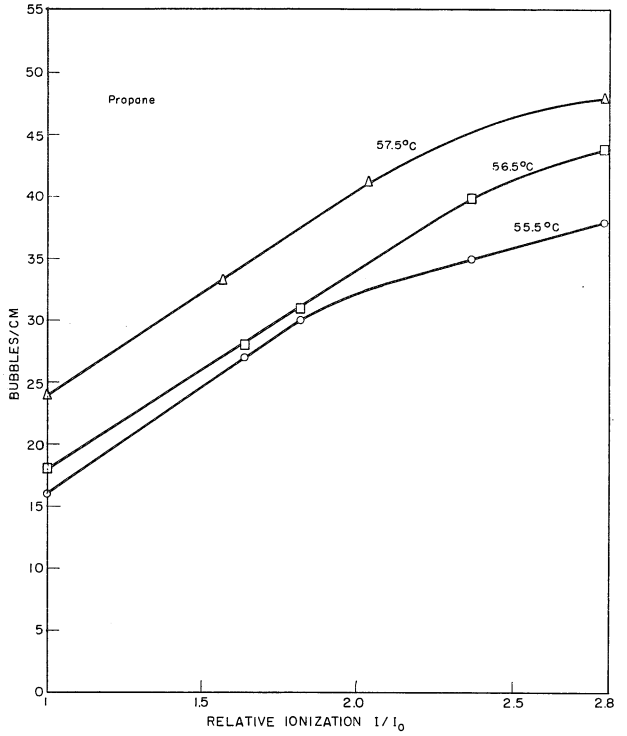

Fig. 6. Observed bubble density in propane versus relative ionization for three temperatures. The bubble density is not linear with relative ionization. Errors are less than 5% in bubble density except for possible temperature variations between runs.

liquid and $\beta = v/c$ for the particle. This formula is valid only when the lower energy limit, E'_1 is at least three times the average ionization potential of the atoms of the liquid, for only in that case can the atomic binding energy of the electrons be neglected as was done in deriving equation (1). In comparing n_δ with the bubble density, we include only those bubbles which lie on the track, and exclude those belonging to a very energetic delta ray that extends some distance away from the track. This procedure leads to an upper limit, $E'_2 \approx 50$ Kev. Since E'_1 is only a few kilovolts, n_δ is not very sensitive to the exact value of E'_2. If we suppose that all delta rays more energetic than E'_1 are able to nucleate a bubble, we expect the bubble density to be proportional to $1/\beta^2$. If we further suppose that changing the temperature changes the threshold delta ray energy required for bubble nucleation, we expect the bubble density, b, to obey to relationship

$$b = C(T)/\beta^2 \quad \text{bubbles/cm} \qquad (2)$$

where C(T) is a function of the temperature, T, through E'_1 and because of the variation of the density of the liquid with temperature.

In fig. 7 we see that the bubble density is indeed a linear function of $1/\beta^2$, although the scatter of points is worse than expected from statistical fluctuations and momentum spread in the beam. The data do not fit equation (2), however, but are fairly well represented by a family of parallel lines described by

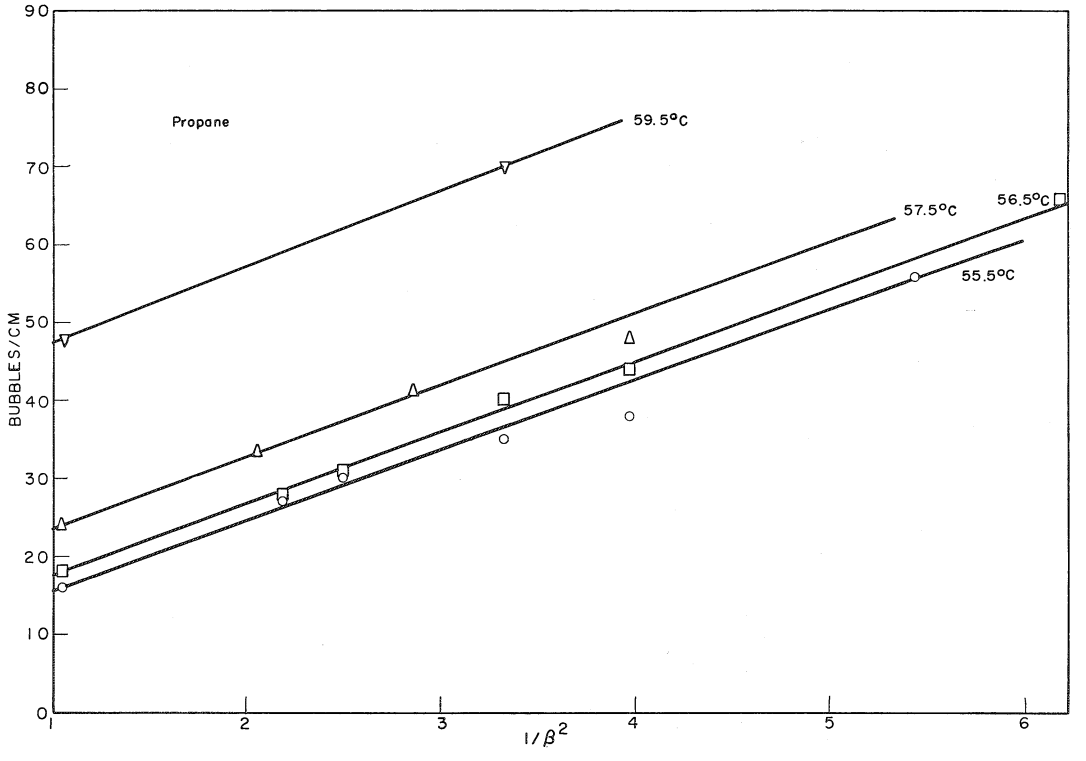

Fig. 7. Observed bubble density in propane versus $1/\beta^2$ for the moving particles. Lines of constant slope fit the data roughly. The scatter of points is probably due to temperature variations between runs. Other errors are less than 5% in bubble density.

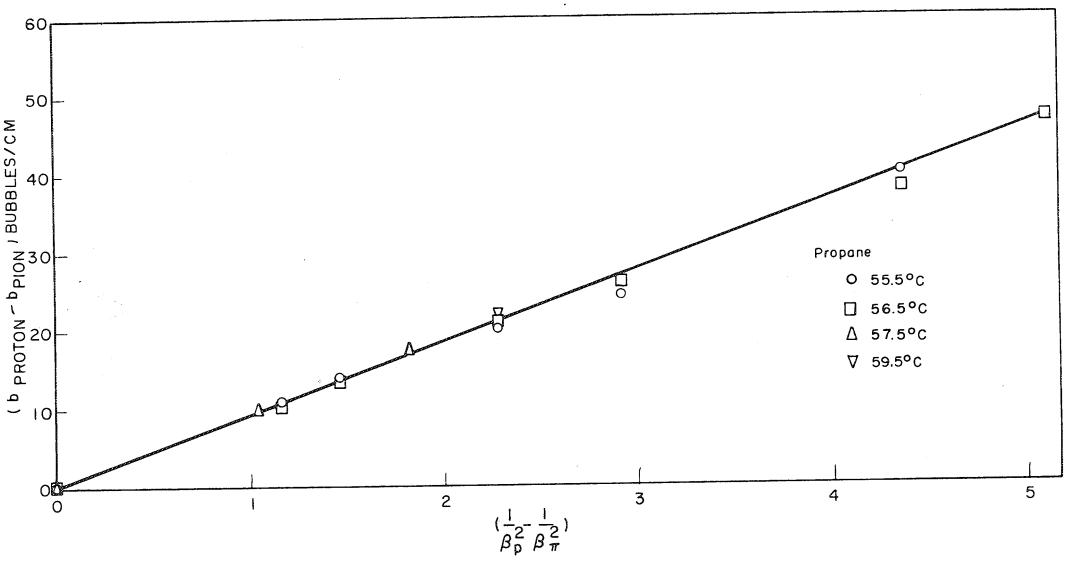

Fig. 8. All the observed densities are reduced to a single straight line by using fast minimum ionizing pions as comparison tracks. This minimizes errors due to temperature fluctuations and provides a temperature-independent means of measuring particle velocities. Errors due to momentum spread in the beam may be 5% for the slower particles.

$$b = A/\beta^2 + B(T) \text{ bubbles/cm} \qquad (3)$$

in which only B is temperature dependent and the slope, A, seems roughly independent of temperature. Since temperature instability was one of the main difficulties in carrying out these measurements because of the extra heat of recompression described above, we believe that some of the scatter of points in fig. 5 is due to temperature variations. During a run at a given momentum the temperature could not have changed much, but from one run to the next at a different momentum, the temperature might have changed.

To reduce this uncertainty due to temperature fluctuations, one can use the tracks of fast particles present in every picture as comparison tracks. This is similar to the use of minimum ionization tracks for standardization and calibration of ionization measurements in cloud chambers and nuclear emulsions. In the case of bubble counting we notice that using equation (3) we can form temperature independent differences

$$b_1 - b_2 = A\,(1/\beta_1^2 - 1/\beta_2^2) \text{ bubbles/cm} \qquad (4)$$

by subtracting the bubble counts of two different tracks in the same picture or run, for which the temperatures are the same. Choosing the fast pions with $\beta \approx 1$ as comparison particles we can plot the bubble density differences according to equation (4). This has been done in fig. 8 in which all the bubble density data taken at 55.5 °C., 56.5 °C., 57.5 °C. and 59.5 °C. reduce quite remarkably to a single universal curve. From fig. 6 we find that $A = 9.2 \pm 0.2$ bubbles/cm for protons in propane. Preliminary measurements at 55 °C. are consistent with this same value of A, but measurements at 54 °C., 53 °C., and 52 °C., indicate that A becomes smaller below 55 °C. At 50 °C. no tracks are visible, at 52 °C. only stopping protons can be seen, and at 53 °C. and 54 °C., minimum ionizing pions make 2.9 bubbles/cm. and 8.1 bubbles/cm. respectively as shown in fig. 3. Our measurements indicate, therefore, that equation (4) is valid with constant A for propane from 55 °C. to 59.5 °C. and for values of $1/\beta^2$ up to about 6. The variation of B(T) with temperature is shown in fig. 9. If equation (4) is found to describe the bubble density at temperatures below 55 °C., A will be less than 9.2 bubbles/cm.

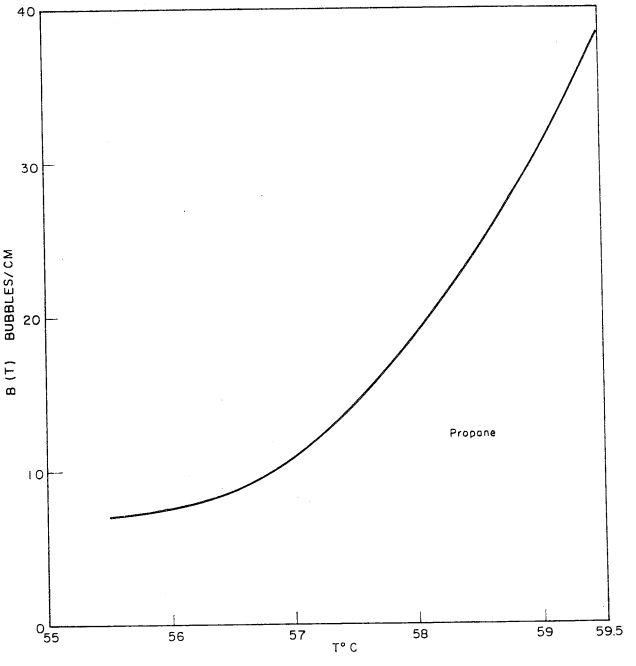

Fig. 9. Temperature-dependent part of the observed bubble density in propane, B(T) = b– $9.2/\beta^2$ bubbles/cm plotted versus temperature. B(T) does not depend on the velocity of the particle making the track.

The explanation of the empirical result expressed by equation (3) must certainly depend on the microscopic mechanism of bubble nucleation by ionizing events. It will involve properties of the liquid and details of the process by which charged particles lose energy in penetrating the liquid. One therefore expects that the values of A and B(T) as well as the range of validity of equation (3) will be different for different liquids. It is important for the interpretation of bubble chamber photographs to know if these numerical results apply to any propane chamber, or whether they depend on the details of the expansion process and therefore apply only to the chamber used in these experiments. We have no direct evidence on this points, except that the existence of a plateau of uniform sensitivity for both the 6-inch chamber used here, and a 2-inch chamber with much different expansion hydrodynamics described previously[1] implies that conditions in the chamber, at least during this brief interval of uniform sensitivity, are not highly dependent on the details of the expansion process. Slight changes in expansion ratio which must have occurred during this experiment do not seem to have affected the results greatly either. Careful calibration with different chambers will settle this question.

V. *Conclusions and applications*

These results suggest a procedure for using bubble counting for determining the velocities of charged particles in nuclear events photographed in bubble chambers. Provision should be made that each picture, or at least a few pictures in each run, have tracks of particles of known velocity. Since the particles will generally be selected by magnetic deflection, fast particles should be used where possible because their velocity is least sensitive to momentum errors. If a number of long calibration tracks are used, the error in the measurement of their bubble densities can be made quite small, as it is limited principally by statistics. Then equation (4) can be used to find the velocity β_1, of the unknown particle from its bubble density b_1. Since A, b_2, and β_2 can be measured very well as described above, the uncertainty in the unknown velocity β_1 will result mainly from the uncertainty in b_1, which is a consequence of statistical fluctuations in the production of bubbles on the unknown track. This procedure is equivalent to determining accurately the values of A and B in equation (3).

We calculate the percent error in β, assuming A and B to be known exactly. From equation (3), we find by taking the absolute value of the logarithmic derivative,

$$\delta\beta/\beta = {}^1/_2 \cdot \delta(b\text{-}B)/(b\text{-}B) = {}^1/_2 \cdot \delta b/(b\text{-}B) \qquad (5)$$

For a track of lengh L centimeters, the standard deviation in the total number of bubbles is $\sqrt{b\,L}$, assuming the bubbles to be formed by random, independent events, since b L is the average total number of bubbles. Then we put $\delta b = \sqrt{bL/L}$ into equation (5) and use equation (3)

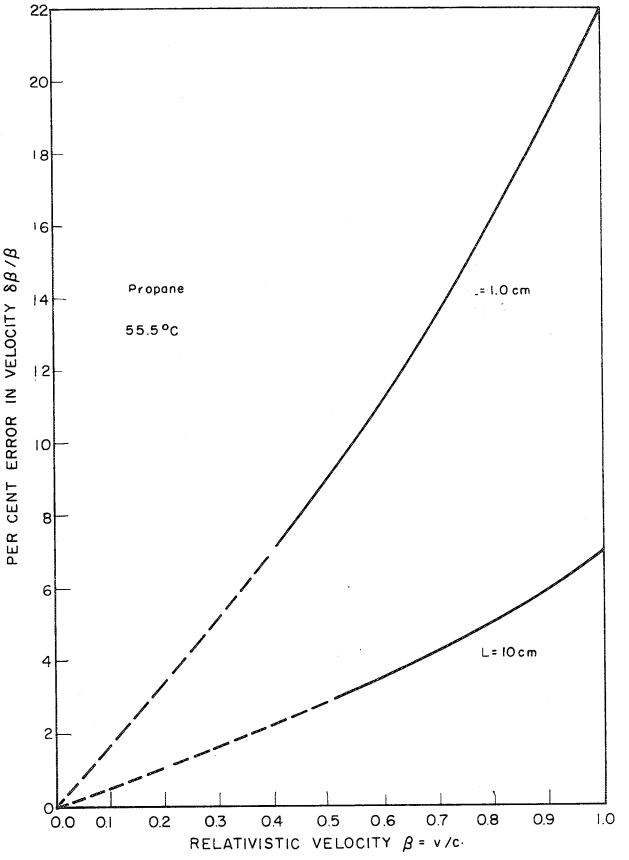

Fig. 10. Percent errors in determining charged particle velocities by bubble counting are plotted versus particle velocity for propane. Only statistical fluctuations in bubble production are considered in these estimates, shown for 1-cm. and 10-cm. track segments. These errors do not apply to slow particles because the bubble density varies along the segment counted. The solid parts of the curves show the approximate region of validity for protons.

to find

$$\delta\beta/\beta = {}^1/_2 \sqrt{b/L} \cdot 1/(b\text{-}B) = \beta/2\sqrt{AL} \cdot \sqrt{1 + \beta^2\, B/A} \qquad (6)$$

We see that the percent error in the velocity varies inversely as the square root of the track length and can be reduced by lowering the temperature to make B(T) smaller. Reduction of the temperature below a certain value is impractical, however, for the bubbles on lightly ionizing tracks become so sparse that the tracks are very difficult to see, and their points of intersection in nuclear collisions become uncertain. On the other hand the bubble densities of very slow particles can be measured reliably only at fairly low temperatures. Some types of observations may therefore require high operating temperatures, while others may be possible only at low temperatures. In fig. 10 are plotted the appropriate percent errors in β calculated from equation (6) for propane at 55 °C. using 10 cm. and 1.0 cm. track lengths. For low velocities shown as dotted portions of the curves, β changes considerably along the track due to the energy loss, even for protons.

When the range-energy relations are known for various particles in propane, it will be possible to take into account variation of bubble density along a track. Bubble density versus residual range will then furnish a means of estimating particle masses.

We are grateful to the Cosmotron staff at the Brookhaven National Laboratory for making these experiments possible, and expecially to the Cloud Chamber Group at the Laboratory for their extensive help in carrying out the exposures.

LIST OF REFERENCES

1. Glaser, D. A. Bubble chambers. *In* Rochester Conference on high energy nuclear physics. 5th. Proceedings, p. 180-1, 1955.
2. Glaser, D. A. and Rahm, D. C. Characteristics of bubble chambers. Phys. Rev., *97*, p. 474-9, 1955.
3. Eisberg, R. (private communication.)
4. Glaser, D. A. and Roellig, L. O. (to be published.)
5. Rahm, D. C. Thesis : University of Michigan, 1956.
6. Glaser, D. A. (to be published.)
7. Rossi, B. High energy particles. New York, 1952, p. 15.

DISCUSSION

A. Rogozinski: Is the percentage of ethylene (2%) in xenon critical?

D. A. Glaser. No, the minimum is probably about 0.1% because there are about 10,000 collisions before an atomic radiation process and the cross-section for superelastic collisions between an excited xenon atom and an ethylene molecule is probably about 0.1 times geometric. Hence about one molecule in 1000 should be hydrocarbon. Apparently xenon and ethylene are completely miscible so that large amounts of ethylene may be added if it is desirable to have many free protons in the liquid for special experiments. We have used 2% by weight of ethylene in our experiments.

G. C. Wick. Is scattering in the xenon chamber so large that the polarization of γ rays cannot be measured?

D. A. Glaser answered that the experiment was tried, to ascertain the parity of the π°, and apparently in nearly pure xenon scattering is too strong.

E. Segrè. Even the absence of heavy particles in a star is not sufficient to ensure that an antiproton has been captured by hydrogen. In photographic emulsions we have observed an antiproton giving rise to a star containing only mesons but in an odd number. Such a star cannot originate from a proton antiproton annihilation.

M. Sands. J. Teem and his co-workers of California Institute of Technology have with the co-operation of the Berkeley group exposed one of the Berkeley hydrogen bubble chambers in the γ-ray beam of the Berkeley synchrotron. The chamber was operated in a magnetic field. It was found that for electrons the mean distance between bubbles, λ, behaves the relation found by Glaser in his work, i.e. $\lambda \simeq 1/\beta^2$.